Düzce University Journal of Science & Technology

Thermodynamic, Economic and Environmental Assessment of Vapor Compression Refrigeration System Using Mono and Binary Nanolubricants (TiO$_2$-B)

[iD] Gökhan YILDIZ [a,*]

[a] *Department of Electronics and Automation, Düzce Vocational School, Düzce University, Düzce, TURKEY.*
* Corresponding author's e-mail address: gokhanyildiz@duzce.edu.tr

ABSTRACT

Nowadays, the need for energy is gaining significant importance. However, energy consumption in developed countries is quite high. Almost 40% of this energy consumption comes from heating, refrigeration, and air conditioning systems in buildings. Hence, even a minor enhancement in refrigeration systems will lead to energy savings on a global scale. Many studies are being conducted for this circumstance. One of these is the addition of nanoparticles to refrigerants and lubricants. In this study, the effects of mono and binary nanolubricants obtained from different nanoparticles (TiO$_2$ and Boron) used at different concentrations (3.5 g/L and 7 g/L) in the vapor compression refrigeration system were evaluated in terms of energy, exergy, environment, and economy. As a result, a 16.47% increase in COP value was obtained in 7 g/L TiO$_2$-B binary nanolubricant compared to pure POE. The energy consumption of the compressor in the system reduced by 13.06% in the 7 g/L TiO$_2$-B binary nanolubricant compared to POE. A 35.20% decrease in total exergy destruction was detected in 7 g/L TiO$_2$-B binary nanolubricant compared to POE. 43.44% increase in exergy efficiency occurred in 7 g/L TiO$_2$-B binary nanolubricant compared to POE in the system. When the system was examined from an economic perspective, a 35.84% improvement was observed in the 7 g/L TiO$_2$ binary nanolubricant compared to POE. When the system was examined environmentally, an 11.90% reduction was achieved in 7 g/L TiO$_2$-B binary nanolubricant compared to POE. As a result, it is seen that significant improvements occur in the system as the concentration increases when mono and binary nanolubricants are used compared to POE.

Keywords: Energy, Environment, Exergy, Binary nanofluid, Vapor compression refrigeration system.

Mono ve İkili Nanoyalayıcı (TiO$_2$-B) Kullanılan Buhar Sıkıştırmalı Soğutma Sisteminin Termodinamik, Ekonomik ve Çevresel Değerlendirmesi

ÖZ

Enerji her geçen gün önemli bir hal almaktadır. Ancak, gelişmiş ülkelerdeki enerji tüketimi oldukça fazladır. Bu enerji tüketiminin neredeyse %40 binalardaki ısıtma, soğutma ve iklimlendirme sistemlerinden kaynaklıdır. Bu nedenle, bu sistemlerde yapılacak olan küçük bir iyileştirme bile küresel boyutta enerji tasarrufuna yol açacaktır. Bu durum için birçok çalışma yapılmaktadır. Bunlardan bir tanesi de soğutucu akışkanlara ve yağlayıcılara nanoparçacık ilave edilmesidir. Bu çalışmada, buhar sıkıştırmalı soğutma sisteminde farklı konsantrasyonlarda (3,5 g/L ve 7 g/L) kullanılan farklı nanoparçacıklardan (TiO2 ve Boron) elde edilen mono ve ikili nanoyağlayıcıların sistem üzerindeki etkileri enerji, ekserji, çevresel ve ekonomik açıdan değerlendirilmiştir. Sonuç olarak, COP değerinde saf POE'ye göre 7 g/L TiO2-B ikili nanoyağlayıcıda %16,47'lik artış elde edilmiştir. Sistemdeki kompresörün enerji tüketiminde saf POE'ye göre 7 g/L TiO2-B ikili nanoyağlayıcıda

%13,06'lık azalma meydana gelmiştir. Toplam ekserji yıkımında saf POE'ye göre 7 g/L TiO2-B ikili nanoyağlayıcıda %35,20'lik azalma tespit edilmiştir. Sisteminde ekserji veriminde saf POE'ye göre 7 g/L TiO2-B ikili nanoyağlayıcıda %43,44'lük artış meydana gelmiştir. Sistem ekonomik açıdan incelendiğinde saf POE'ye göre 7 g/L TiO2 ikili nanoyağlayıcıda %35,84'lük iyileşme gözlenmiştir. Sistem çevresel olarak incelendiğinde saf POE'ye göre 7 g/L TiO2-B ikili nanoyağlayıcıda %11,90'lık azalma gerçekleşmiştir. Sonuç olarak, saf POE'ye göre mono ve ikili nanoyağlayıcılar kullanıldığında konsantrasyon arttıkça sistem üzerinde önemli iyileşmeler meydana geldiği görülmektedir.

Anahtar Kelimeler: Enerji, Çevre, Ekserji, İkili nanoakışkan, Buhar sıkıştırmalı soğutma sistemi

I. INTRODUCTION

Today, in industrialized countries, a portion of electricity consumption is used in cooling applications. The market volume of the heating, ventilation, and air conditioning (HVAC) sector is expected to reach 241.8 billion dollars in 2025 [1]. HVAC systems account for a large portion of energy consumption in buildings. For example, it is known that more than 50% of total building energy consumption in the United States comes from HVAC applications [2]. In Australia, it has been determined that HVAC applications are responsible for 20-50% of the total energy used in buildings. In household refrigeration systems, it is generally used for the preservation of food products and air conditioning of spaces. It is estimated that approximately 1.5 billion household refrigerators are used in the world. Commercial refrigeration devices are used in various industrial applications, especially in the storage of foods. According to the World Refrigeration Organization, it is estimated that there are 90 million commercial refrigeration devices in operation worldwide [3]. In China, 1% of the population had air conditioning in 1990, while 100% of the population had air conditioning in 2009 [4]. Approximately 17% of electricity in the world is used in refrigeration applications and 45% of this is used in buildings [5]. The International Energy Agency's 2050 technology roadmap recommends using more efficient systems that will simultaneously produce heating, cooling, and hot water for buildings.

The usage of nanofluids has become widespread with the development of nanotechnology to increase efficiency in cooling and heating systems in recent years. To increase performance in cooling systems, nanoparticles are added to refrigerants and lubricants and used as nanorefrigerants and nanolubricants. Nanolubricants are obtained by adding nanoparticles to the lubricant. The resulting nanolubricant is then placed into the compressor. Nano refrigerants are obtained by directly mixing conventional refrigerants and nanoparticles. The most important reason for adding nanoparticles to liquids is that solid-phase materials have higher thermal properties than lubricants and refrigerants. This will increase the thermal properties of the liquids used in the cooling system [6, 7]. As a result, it improves the thermal performance of most systems requiring high heat transfer [8, 9].

Zawawi et al. studied the performance of Al_2O_3-SiO_2/PAG binary nanolubricants at a 60:40 composition ratio at different concentrations (0.005-0.06% by volume) on automotive air conditioning system. The experiments were carried out with a charge of 95-155 g R134a and different compressor speeds between 900-2100 rpm [10]. Chauhan performed performance analysis in an ice machine using R134a as refrigerant, PAG46 as lubricant, and binary nanoparticles (Al_2O_3-SiO_2) with concentrations ranging from 0.02% to 0.1%. The lowest compressor power and highest COP were observed at 0.08% concentration. Compressor power consumption was 6.8% and 3.5% higher for binary nanolubricants than for mono nanolubricants, Al_2O_3, and SiO_2, respectively. It was determined that the COP value of binary nanolubricants at 0.08% volume concentration was 10.89% and 5.3% higher than Al_2O_3 and SiO_2 mono nanolubricants, respectively [11]. Wanatasanappan et al. studied the thermophysical performances of Al_2O_3-CuO binary nanolubricants at different mixing ratios (20:80, 40:60, 50:50, and 60:40) at 1% concentration. Thermal conductivity and viscosity measurements were carried out between 30 and 70 °C. The highest thermal conductivity for Al_2O_3-CuO nanofluid was obtained in the 60:40 mixture with a 12.33% increase compared to the reference fluid. Additionally, the viscosity of

the hybrid nanofluid showed a decreasing trend with increasing temperature [12]. Zawawi et al. studied the thermophysical properties of Al_2O_3-SiO_2/PAG binary nanolubricants at concentrations of 0.02 to 0.1 vol. C between temperatures of 303 and 353 K. These nanolubricants used in the experiments behaved as Newtonian fluids in these temperature ranges. The highest thermal conductivity increase was obtained as 2.41% at 0.1% concentration and 303 K temperature. The viscosity value was observed to improve by 9.71% at 0.1% concentration and 333 K temperature [13]. Asokan et al. studied the thermophysical properties such as thermal conductivity, viscosity, density, and specific heat capacity of low-concentration hybrid nanofluids. These thermophysical properties were compared in low-concentration mono and hybrid nanofluids. Mono and hybrid nanofluids were prepared at concentrations of 0.02%, 0.04%, and 0.06%. The results obtained showed that the thermal conductivities of hybrid nanofluids were higher than those of mono nanofluids. The thermal conductivity of Al_2O_3-CuO nanofluid increased by 2.3% compared to CuO and 3.6% compared to Al_2O_3 [14]. Senthilkumar et al. performed performance evaluation in a vapor compression refrigeration system (VCRS) using 40 and 60 g of R600a refrigerant with Al_2O_3-SiO_2 nanolubricant at concentrations of 0.4 g/L and 0.6 g/L. As a result of the experiments, a 30% increase in performance, a 25% increase in cooling capacity, and an 80 W decrease in power consumption were achieved [15]. Senthilkumar et al. performed performance analysis in a VCRS using binary nanolubricant consisting of CuO and SiO_2 nanoparticles at concentrations of 0.2 g/L and 0.4 g/L and 40 and 60 g of R600a refrigerant. CuO-SiO_2 binary nanolubricants resulted in a 35% reduction in COP, 18% in cooling capacity, and 75 W in compressor energy consumption [16]. Kumar and Rajput investigated the performance of a VCRS using different concentrations (0.1, 0.2, 0.3, and 0.4 g/L) of TiO_2-SiO_2/MO nanolubricant and different amounts (80, 100 and 120 g) of R600a. Under optimum conditions, a 37.83% improvement in the COP value of the refrigeration system with 80 g R600a was detected. A 13.46% reduction in compressor energy consumption was observed in the system using 80 g R600a. The highest value of exergy efficiency and the lowest value of exergy loss were obtained with 77% and 96.90 W values, respectively, at a concentration of 0.2 g/L in the system using 100 g R600a [17]. Akhtar and Rajput performed performance evaluation in a VCRS using multi-walled carbon nanotube (MWCNT)-Graphene sheets (GN) nanolubricant and 200 g R134a at different concentrations (0.3, 0.5, 0.7 and 0.9 g/L). Hybrid nanolubricant was prepared in the ratio of 50:50. Experimental results showed that compressor power consumption and pressure ratio decreased by 16.09% and 5.68%, respectively. An increase of 11.29% was determined in the COP value of 0.7 g/L hybrid nanolubricant compared to pure POE [18]. Govindasamy et al. investigated the performance of refrigeration systems with normal and microchannel condensers with and without nanoparticles. Experiments were carried out using CeO_2-ZnO hybrid nanolubricants prepared at different ratios (0.5:1.5, 1:1, and 1.5:0.5) and R134a refrigerant. As a result of the experiments, a 33.3% increase in the COP value of the refrigeration system containing a 1:1 binary nanolubricant microchannel condenser was achieved [19].

Approximately 35-40% of the world's energy consumption comes from heating, cooling, and air conditioning systems in buildings. Nowadays, since energy has become very important, it has become necessary to increase energy efficiency in these systems. The best solution to solve this circumstance is to make improvements that will reduce the energy consumption of the system. Studies show that the compressor plays the biggest role in energy consumption in refrigeration and heating systems. Therefore, improvements that can decrease the compressor's energy consumption will specify meaningful energy savings, considering that this circumstance is implemented worldwide. This study focuses on the effects of using TiO_2 and Boron (B) mono and binary nanolubricants at different concentrations (3.5 g/L and 7 g/L) in a VCRS on system performance. In this study, TiO_2 was chosen as the nanoparticle because it was mentioned in the literature that it gave good performance, and the B nanoparticle was chosen because it showed good performance in thermal systems but was determined to be used less in refrigeration systems. The results of energy, exergy, enviroeconomic, and thermoeconomic analyses of TiO_2-B mono and binary nanolubricants at different concentrations in the VCRS were compared with the base fluid.

II. MATERIAL and METHODS

This section includes theoretical explanations and equations of the first and second laws of thermodynamics, environmental analysis, and economic analysis used to evaluate the performance of the VCRS. Additionally, the preparation and thermophysical properties of mono and binary nanolubricants to be utilized in the VCRS are given. In addition, the schematic representation of the VCRS used in the experiments, its technical specifications, and the preparation of the experiments are generally mentioned.

A. NANOFLUID PREPARATION

POE, TiO_2, and B nanoparticles were utilized to obtain mono and binary nanolubricants in this study. The nanoparticles utilized in the experiments were supplied by Nanografi Co, Türkiye. Some technical properties of these nanoparticles are shown in Table 1.

Table 1. Some technical properties of nanoparticles (taken by supplier).

Nanoparticle	Purity, %	Density, g/cm³	Average Particle Size, nm	Morphology	Thermal Conductivity, W/m.K
TiO_2	+99.5	4.5	45	Nearly Spherical	8
B	+99.5	3.58	100	Nearly Spherical	27

As given in Table 1, the shapes of the nanoparticles used in the experiments are close to spherical and their sizes vary between 45 and 100 nm. SEM images are given in Figure 1 to see the chemical structures of the nanoparticles. SEM images were taken at 1 μm size from the FEI brand Quanta FEG 250 model device located at Düzce University laboratories.
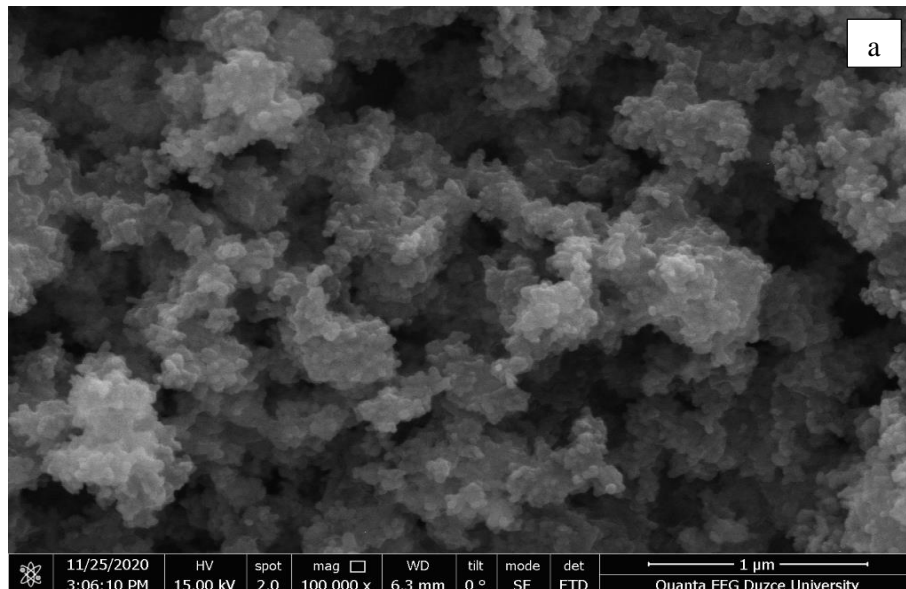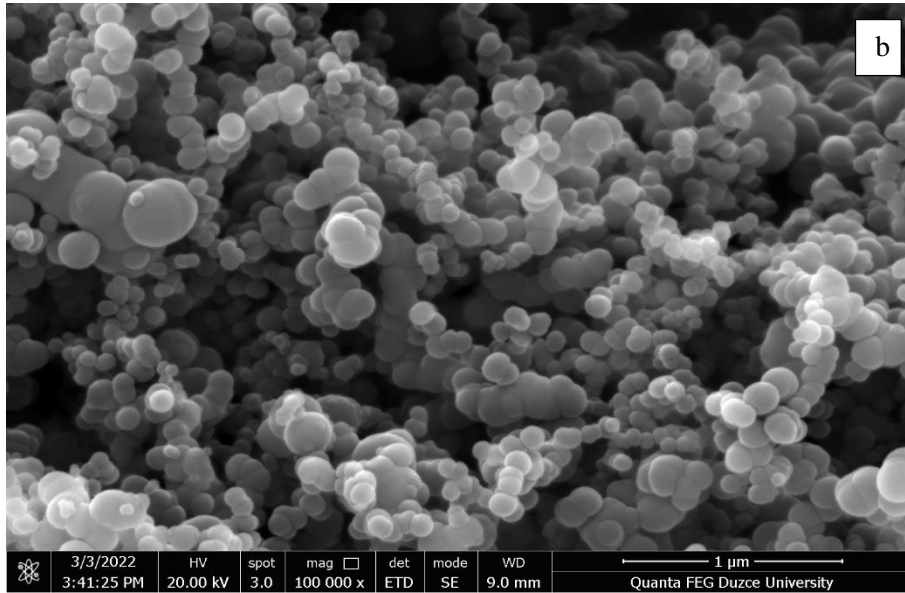
Figure 1. *SEM photos of nanoparticles a) TiO₂, and b) B.*

A precision balance was utilized to measure the masses of POE and nanoparticles. POE, mono, and binary nanoparticles were blended with a mechanical stirrer at 25 °C for 2 h. They were subjected to ultrasonic bath treatment at 50 Hz frequency and 250 W power for 2.5 hours under laboratory conditions to ensure homogeneous distribution of nanoparticles in the POE base fluid. All steps in the preparation of mono and binary nanolubricants are shown in Figure 2.
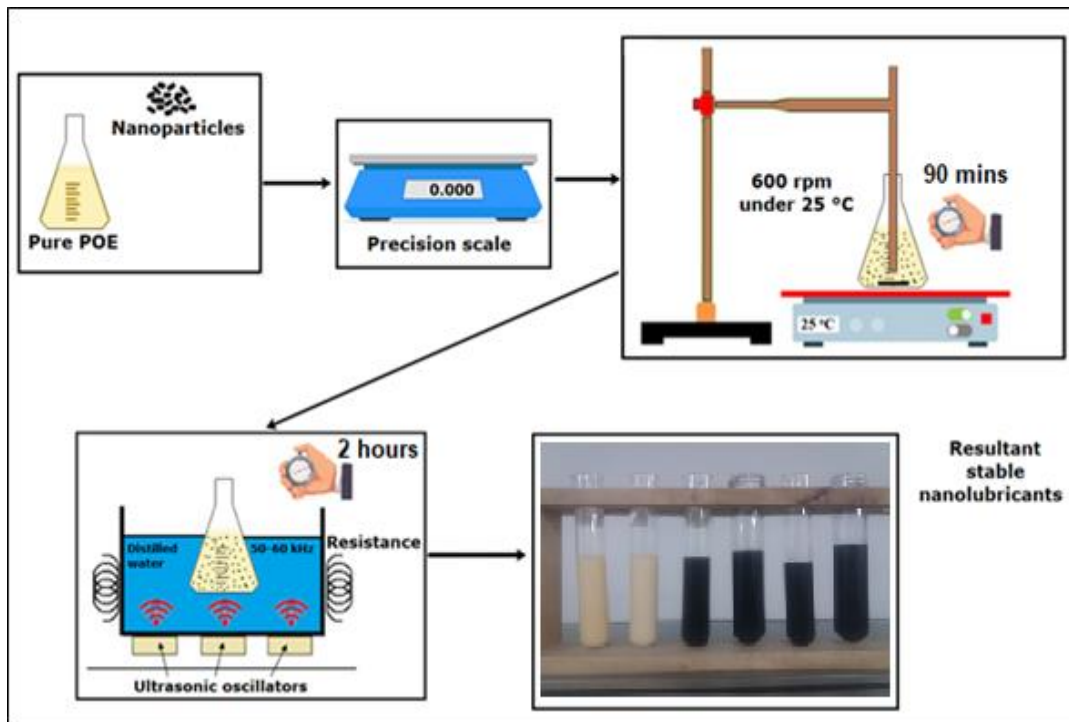

Figure 2. *Steps of preparation of mono and binary nanolubricants.*

B. EXPERIMENTAL SETUP

VCRSs are the most commonly utilized refrigeration systems in practical applications. The mechanical VCRS consists of four main components: compressor, condenser, expansion valve, and

evaporator. In VCRSs, refrigerants are utilized to complete the cycle. In this study, R134a, used in refrigeration applications, was utilized as the refrigerant. The schematic representation of the test rig is given in Figure 3.
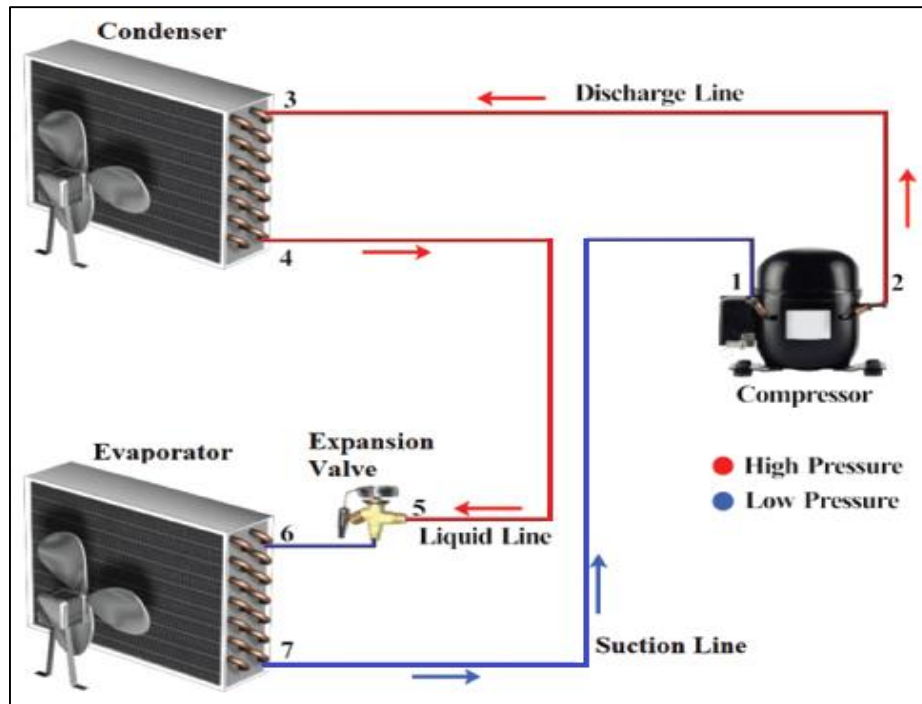

Figure 3. *Schematic view of VCRS*

Before starting the experiments on the VCRS, leak tests were performed. N_2 was charged to the VCRS at 18 bar pressure to determine if there was a leak. To make the leak test more effective, the system was left at this pressure for 1 day. It was determined that there was no change in the pressure values in the system after 1 day. After determining that there were no leaks, 170 g of R134a and 200 mL of POE were added to the VCRS. After the specified amount of POE and refrigerant were charged into the system, the system was operated until it reached equilibrium conditions. When the system reached equilibrium conditions, data were taken at 10-minute intervals for 1 hour. The same methods were applied for other mono and binary nanolubricants (3.5 g/L TiO_2, 7 g/L TiO_2, 3.5 g/L B, 7 g/L B, 3.5 g/L TiO_2-B and 7 g/L TiO_2-B). The tests were carried out at an average of 60% relative humidity and 22 °C ambient temperature conditions. While changing the nanolubricant, the refrigerant was discharged and recharged. Even if the refrigerant is thoroughly drained from the system, there is a possibility that refrigerant may remain in some areas within the system. Therefore, the system was purged with N_2 for approximately 2-3 minutes before refrigerant charging. Refrigerant charging was carried out after this procedure. The experiments were repeated three times for reliability. The technical properties of the VCRS utilized in the experiments are shown in Table 2.

Table 2. *Technical specifications of VCRS*

Components	Specifications
Compressor	Displacement: 4.05-9.09 cm^3 Cooling capacity: 325-970 W
Evaporator	Capacity: 1 kW
Condenser	Capacity: 1.4 kW

Table 2 (cont). Technical specifications of VCRS

Thermostatic expansion valve	Temperature range: -40/10 °C Static superheat: 4 °C
Filter drier	Temperature range: -40/70 °C Net volume: 0.464 L

C. THERMODYNAMIC ANALYSIS

In this study, thermodynamic analyses were applied to investigate the performance of mono and binary nanolubricants utilized in the VCRS. Various energy and exergy methods were considered while applying thermodynamic analyses. Thermal equilibrium equations were applied for each system component.

The amount of heat transferred per unit of time from the evaporator ($\dot{Q}_{evap}$) in the VCRS is calculated in Equation 1.

$$\dot{Q}_{evap} = \dot{m}_r(h_7 - h_6) \tag{1}$$

The amount of heat released from the condenser ($\dot{Q}_{cond}$) in the refrigeration system per unit time is calculated in Equation 2.

$$\dot{Q}_{cond} = \dot{m}_r(h_4 - h_3) \tag{2}$$

Depending on the mechanical and electrical efficiency, the compressor capacity and compressor electrical power are given in Equation 3 and Equation 4.

$$\dot{W}_{comp} = \dot{m}_r(h_2 - h_1) \tag{3}$$

$$\dot{W}_{comp,el} = \frac{\dot{W}_{comp}}{\eta_{mech} \times \eta_{el}} \tag{4}$$

COP represents the electrical power consumed by the compressor. It corresponds to the heat transferred from the evaporator per unit of time. COP is calculated as in Equation 5.

$$COP = \frac{\dot{Q}_{evap}}{\dot{W}_{comp,el}} \tag{5}$$

It is important to determine the energy availability in VCRSs. Therefore, exergy analysis is necessary. The exergy for the steady flow control volume is given in Equation 7. $E_{x,dest}$ in the equation represents exergy destruction. The first two terms in the equation express the flow exergy, the next term expresses the heat transfer exergy, and the last two terms express the work exergy. In the equations, subscripts represent the input and output conditions.

$$E_{x,dest} = \sum \dot{E}_{x,in} - \sum \dot{E}_{x,out} + \sum \left[\dot{Q} \left(1 - \frac{T_0}{T} \right) \right]_{in} - \sum \left[\dot{Q} \left(1 - \frac{T_0}{T} \right) \right]_{out} + \sum \dot{W}_{in} - \sum \dot{W}_{out} \tag{7}$$

The flow exergy for each cycle in the VCRS is given in Equation 8.

$$\dot{E}_x = \dot{m}_r[h - h_0 - T_0(s - s_0)] \tag{8}$$

The general expression of exergy destruction for the compressor is given in Equation 9 and Equation 10.

$$\dot{E}_{x,dest,comp} = \dot{E}_{x,1} - \dot{E}_{x,2} + \dot{W}_{comp,el} \tag{9}$$

$$\dot{E}_{x,dest,comp} = \dot{m}_r[(h_1 - T_0 s_1) - (h_2 - T_0 s_2)] + \dot{W}_{comp,el} \tag{10}$$

The general expression of exergy destruction for the condenser is given in Equation 11 and Equation 12.

$$\dot{E}_{x,dest,cond} = \dot{E}_{x,3} - \dot{E}_{x,4} - \left[\dot{Q}_{cond}\left(1 - \frac{T_0}{T_{cond}}\right)\right] \tag{11}$$

$$\dot{E}_{x,dest,cond} = \dot{m}_r[(h_3 - T_0 s_3) - (h_4 - T_0 s_4)] - \left[\dot{Q}_{cond}\left(1 - \frac{T_0}{T_{cond}}\right)\right] \tag{12}$$

The exergy destruction for the evaporator is given in Equation 13 and Equation 14.

$$\dot{E}_{x,dest,evap} = \dot{E}_{x,6} - \dot{E}_{x,7} + \left[\dot{Q}_{ev}\left(1 - \frac{T_0}{T_{evap}}\right)\right] \tag{13}$$

$$\dot{E}_{x,dest,evap} = \dot{m}_r[(h_6 - T_0 s_6) - (h_7 - T_0 s_7)] + \left[\dot{Q}_{evap}\left(1 - \frac{T_0}{T_{evap}}\right)\right] \tag{14}$$

The exergy destruction of the expansion valve is given in Equation 15 and Equation 16.

$$\dot{E}_{x,dest,exv} = \dot{E}_{x,5} - \dot{E}_{x,6} \tag{15}$$

$$\dot{E}_{x,dest,exv} = \dot{m}_r T_0 (s_6 - s_5) \tag{16}$$

The total exergy destruction caused by all system components is calculated in Equation 17.

$$\dot{E}_{x,dest,overall} = \dot{E}_{x,dest,comp} + \dot{E}_{x,dest,cond} + \dot{E}_{x,dest,evap} + \dot{E}_{x,dest,exv} \tag{17}$$

D. ENVIROECONOMIC ANALYSIS

Fossil fuels, which are predominantly used in energy production, increase the amount of CO_2 released into the atmosphere. Increasing amount of CO_2 in the atmosphere causes problems such as global warming and environmental pollution. Different measures are being taken to solve these problems and reduce CO_2 emissions around the world. The environmental cost analysis carried out in line with this goal is based on the CO_2 emission price. In this study, the amount of CO_2 reduction provided by the VCRS using mono and binary nanolubricants at different concentrations is given in Equation 19.

$$W_{comp,el} = \dot{W}_{comp,el} \cdot t \tag{18}$$

$$\phi_{CO_2} = \psi_{CO_2} \times W_{comp,el} \tag{19}$$

In Equation 19, ϕ_{CO_2} is the amount of CO_2 emissions reduced by the system, and ψ_{CO_2} is the amount of CO_2 produced by the operation of coal-fired power plants. The value of ψ_{CO_2} is taken as 2.08 $kgCO_2/kWh$ [20, 21]. The environmental cost value of the system is calculated in Equation 20.

$$Z_{CO_2} = z_{CO_2} \cdot \varphi_{CO_2} \tag{20}$$

In Equation 20, z_{CO_2} represents the international carbon price and varies between 13 and 16 $/tCO$_2$. The value of z_{CO_2} was taken as 14.5 $/tCO$_2$ in the calculations [22].

E. ECONOMIC ANALYSIS

The economic viability of an energy system can be assessed by calculating some economic indicators such as the cost of useful products over the facility life and the payback period. In such an analysis, the costs of components and other expenses have to be estimated to find out the total revenue requirement. For simplifications, smoothed costs can be used instead of taking the cost change from year to year. Thermoeconomic analysis combines the principles of economic and thermodynamic analysis (usually exergy analysis). The analysis called exergoeconomic analysis is divided into two categories: cost accounting and optimization-based approaches.

The annual operating cost (ARC) of the system is given in Equation 21. $\dot{m}$ in the equation represents the mass flow rate of the refrigerant in the VCRS.

$$ARC = (\dot{m}\Delta P/\rho)t_{op}.CE \tag{21}$$

The present value of an annuity is the monetary value of the total annual payment at the end of a certain period if it had been invested at the beginning of the annuity with the effective interest rate. The initial investment cost recovery factor (CRF) is calculated in Equation 22 [23].

$$CRF = \frac{i(1+i)^n}{(1+i)^n - 1} \tag{22}$$

In Equation 22, n is the service life of the VCRS and i is the assumed annual interest. The life of the experimental system is 20 years [24] and the assumed annual interest is 10% [25]. The first annual cost (FAC) is calculated as in Equation 23.

$$FAC = CRF \times TCI \tag{23}$$

TCI in the equation represents the initial investment cost.

$$SFF = \frac{i}{(1+i)^n - 1} \tag{24}$$

In Equation 25, ASV represents the annual scrap value, SFF represents the depreciation fund factor, and SV represents the scrap value of the system.

$$ASV = SFF \times SV \tag{25}$$

$$SV = \mu \times TCI \tag{26}$$

Annual maintenance cost (AMC) was used in the calculations as 10% of the initial investment cost [26]. In the equation, AC represents the annual cost.

$$AC = FAC + AMC + ARC - ASV \tag{27}$$

$$R_{g,ex} = \frac{\dot{E}x_{out}}{AC} \tag{28}$$

F. UNCERTAINTY ANALYSIS

The method called uncertainty analysis is used for error analysis of experimental data. According to this method, let the quantity to be measured in the system be R and the n independent variables

affecting this quantity be $x_1, x_2, x_3, \ldots, x_n$. In this case, $R = R(x_1, x_2, x_3, \ldots, x_n)$ can be written. If the error rates for each independent variable are $w_1, w_2, w_3, \ldots, w_n$ and the ratio of the R magnitude is W_R, the uncertainty analysis can be written as Equation 29. Total uncertainty is 1.21%.

$$W_R = \left[\left(\frac{dR}{dx_1} w_1 \right)^2 + \left(\frac{dR}{dx_2} w_2 \right)^2 + \cdots + \left(\frac{dR}{dx_n} w_n \right)^2 \right]^{1/2} \tag{29}$$

Table 3. *Specifications of the measurement devices.*

No.	Measurement Instrument	Range	Accuracy
1	Thermocouple (K type)	(-30)-130 °C	0.5%
2	Radwag precision scales	0-220 g	0.001 g
3	Energy meter	0.1-3680 W	0.1 W
4	Pressure transmitter	0-30 bar	1 bar

III. RESULTS and DISCUSSION

In this section, the system performance of the VCRS using different concentrations of mono and binary nanolubricants was investigated and interpreted in terms of energy, exergy, environment and economy. Experimental data were taken at 10 minute intervals for 1 hour after the system reached equilibrium. Experiments were conducted at approximately 22 °C and 60% relative humidity.

Compressor energy consumption of mono and binary nanolubricants at different concentrations used in the VCRS is given in Figure 4. As seen in Figure 4, it was observed that the energy consumption of the compressor decreased significantly as the concentrations of mono and binary nanolubricants increased compared to pure POE. While the compressor energy consumption in pure POE was 392.97 W, the lowest energy consumption was obtained as 341.64 W in 7 g/L TiO_2-B/POE nanolubricant. This is because the nanoparticles used in the VCRS are approximately spherical in shape and exhibit a rolling effect, acting as a bearing of nanoparticles to reduce power loss [27]. Nanoparticles exhibit ball bearing behavior to reduce power loss caused by the reduction of friction between mating surfaces because of the rolling effect. Additionally, heat transfer between fluids increases due to the high thermal conductivity values of nanolubricants [28, 29]. In this case, it is a parameter that reduces the energy consumption.
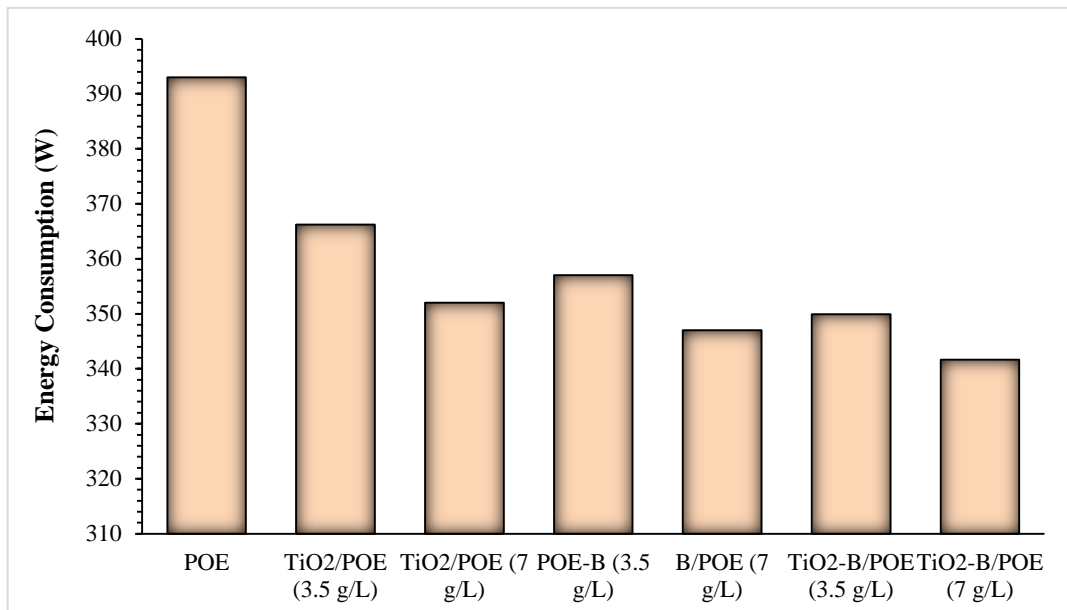
Figure 4. *Energy consumption of mono and binary nanolubricants at different concentrations*

COP changes of mono and binary nanolubricants at different concentrations used in the VCRS are given in Figure 5. There is a significant increase in the COP values of mono and binary nanolubricants compared to pure POE as the concentration increases. While the lowest COP value was 3.4 in pure POE, the highest COP value was determined in 7 g/L TiO$_2$-B/POE nanolubricant. One of the most important factors that cause the COP value to be higher in mono and binary nanolubricants compared to POE is low energy consumption. As seen in the COP formula, cooling capacity and energy consumption play a major role in the COP value. Therefore, due to the thermophysical properties of mono and binary nanolubricants, reducing friction in the compressor and having high thermal conductivity, the energy consumption is lower than the compressor energy consumption in the system using pure POE. In addition, the cooling capacities in mono and binary nanolubricants are higher than those in pure POE, which is another reason why the COP value is high. This result shows that increasing the fraction of binary nanolubricants used in the VCRS has higher efficiency compared to pure POE.
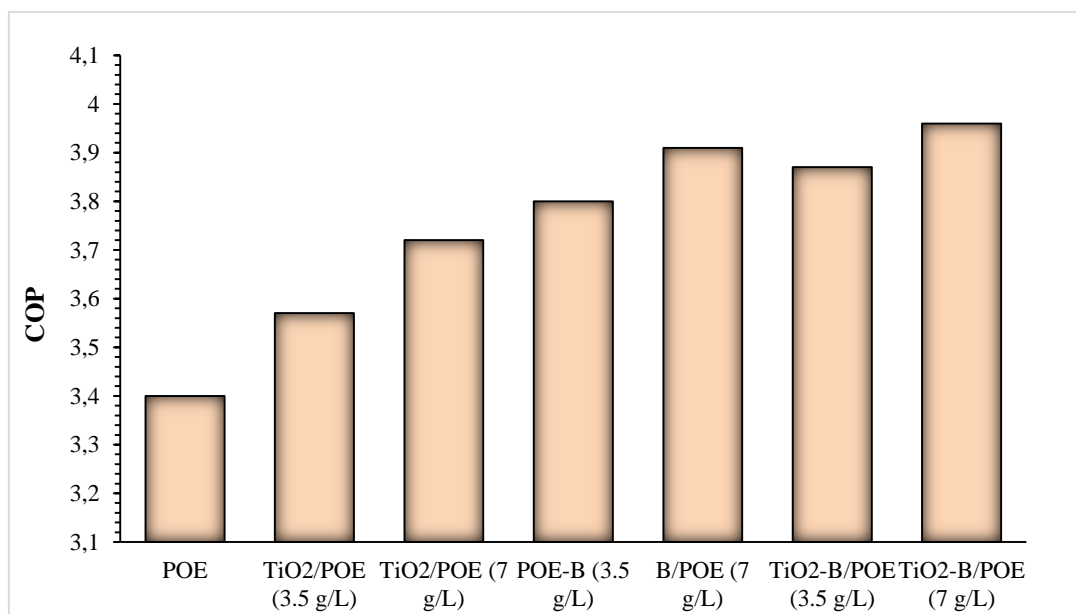

Figure 5. *COP values of mono and binary nanolubricants at different concentrations*

The total exergy destruction of pure POE, mono and binary nanolubricants at different concentrations in the VCRS is shown in Figure 6. The total exergy destruction of mono and binary nanolubricants decreases as the concentration enhances compared to pure POE. The lowest total exergy destruction was obtained as 618.696 W in pure POE, while the highest total exergy destruction was obtained as 400.924 W in 7 g/L TiO_2-B/POE. As seen in the figure, as the concentrations of mono and binary nanolubricants enhance, the type of nanolubricants in the VCRS becomes clear.
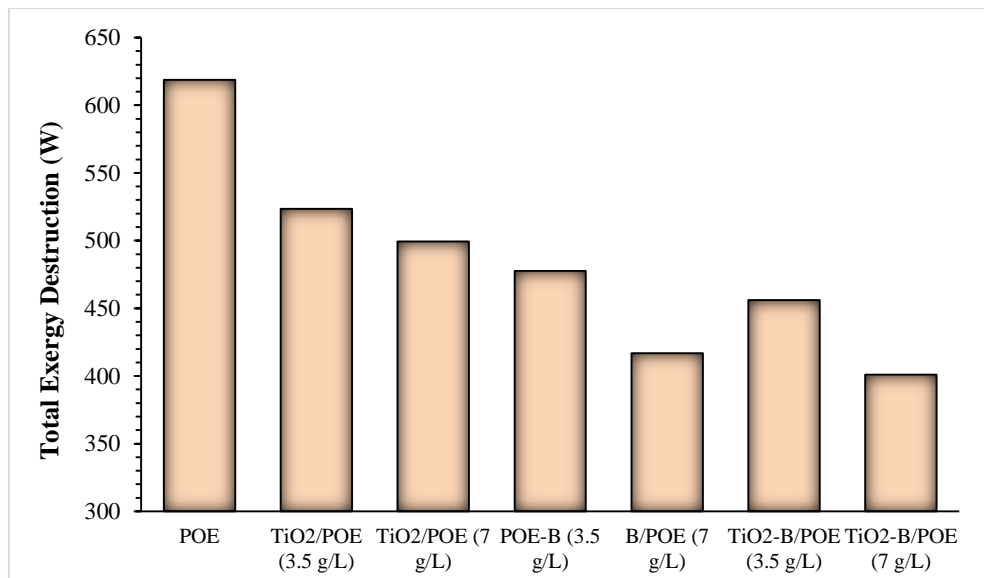

Figure 6. Total exergy destruction of mono and binary nanolubricants at different concentrations

The exergy efficiencies of POE, mono and binary nanolubricants at different concentrations in the VCRS are given in Figure 7. Exergy efficiency increases as the concentrations of mono and binary nanolubricants increase compared to pure POE. The lowest exergy efficiency was obtained with 34.53% in pure POE, and the highest exergy efficiency was determined with 49.53% in 7 g/L TiO_2-B/POE. As seen in Figure 5, the trend in COP changes is similar to the second law efficiency. This can be explained as the role of enhancing nanoparticle amount due to increased heat transfer with enhancing concentration. The thermal properties of nanolubricants that need to be taken into account can also be well understood at high concentrations.
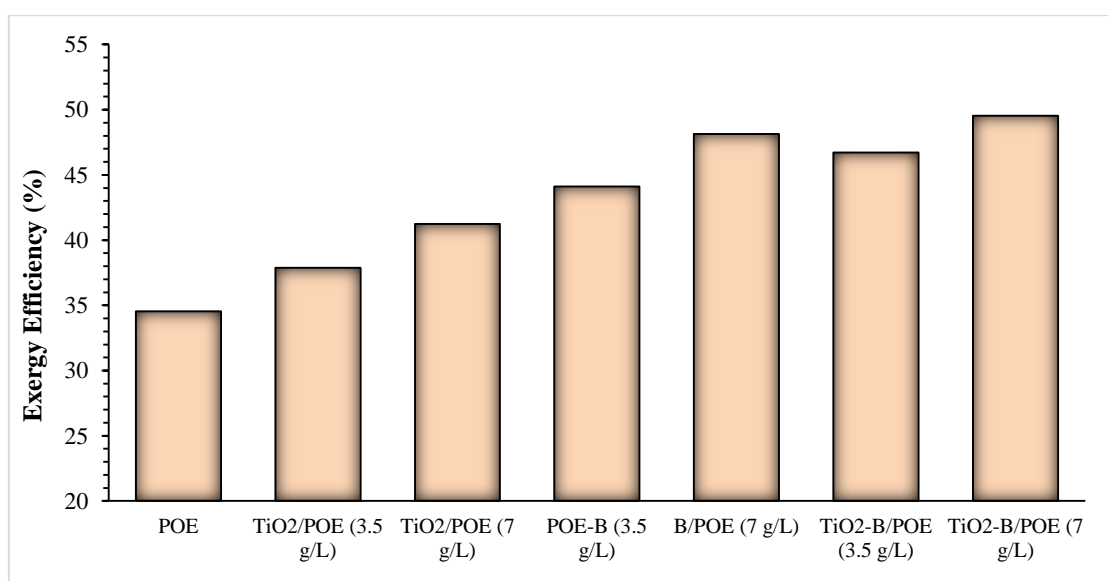

Figure 7. Exergy efficiencies of mono and binary nanolubricants at different concentrations

Today, the environmental potential of thermal energy systems is as important as the efficiency of the systems due to the effects of global warming. The emission pricing in the VCRS using POE, mono and binary nanolubricants to provide environmental vision is shown in Figure 8. The highest amount obtained per CO_2 emitted was 0.21 ¢/h in pure POE, while the highest amount was 0.185 ¢/h. Since this amount is calculated based on the amount of energy consumed by the system, it is parallel to the energy consumption trend in Figure 4.
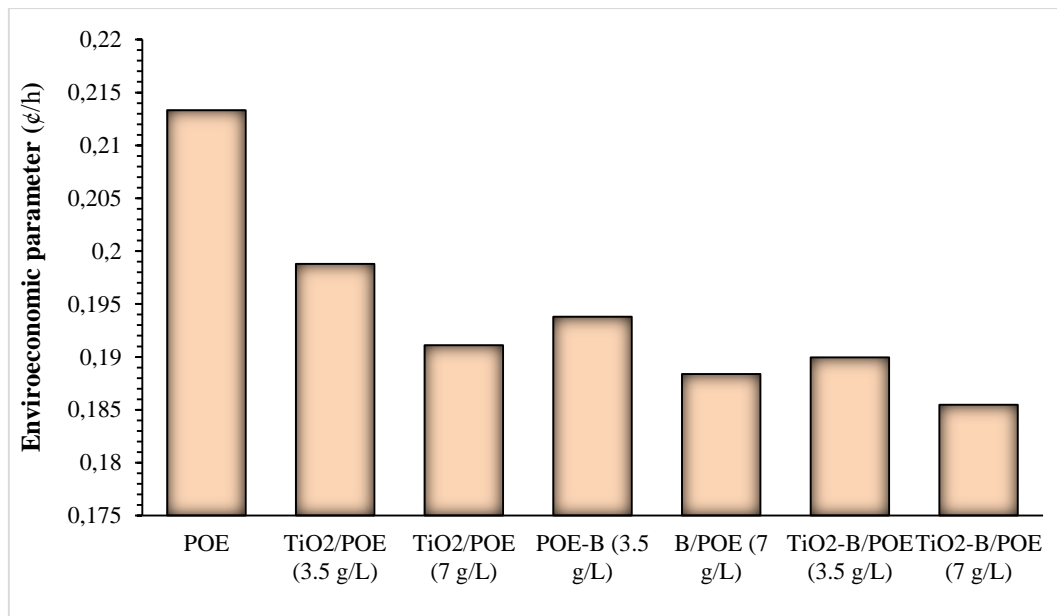

Figure 8. *Enviroeconomic values of mono and binary nanolubricants at different concentrations*

Evaluating a system in terms of economy is as important as improving the performance of the system. The economic comparison of pure POE, mono and binary nanolubricants used in VCRS is given in Figure 9. As seen in the figure, the worst economic performance was obtained with 1.409 kWh/$ in pure POE, while the best economic performance was obtained with 0.904 kWh/$ in 7 g/L TiO_2-B/POE nanolubricant. In the VCRS, energy consumption decreases as the concentrations of mono and binary nanolubricants increase compared to pure POE, and accordingly the economic cost decreases in direct proportion. According to Figure 9, the $R_{g,ex}$ values of mono and binary nanolubricants gave better results than POE. The reason for this can be explained as the increase in exergy efficiency and the decrease in exergy destruction when mono and binary nanolubricants are utilized in the VCRS.
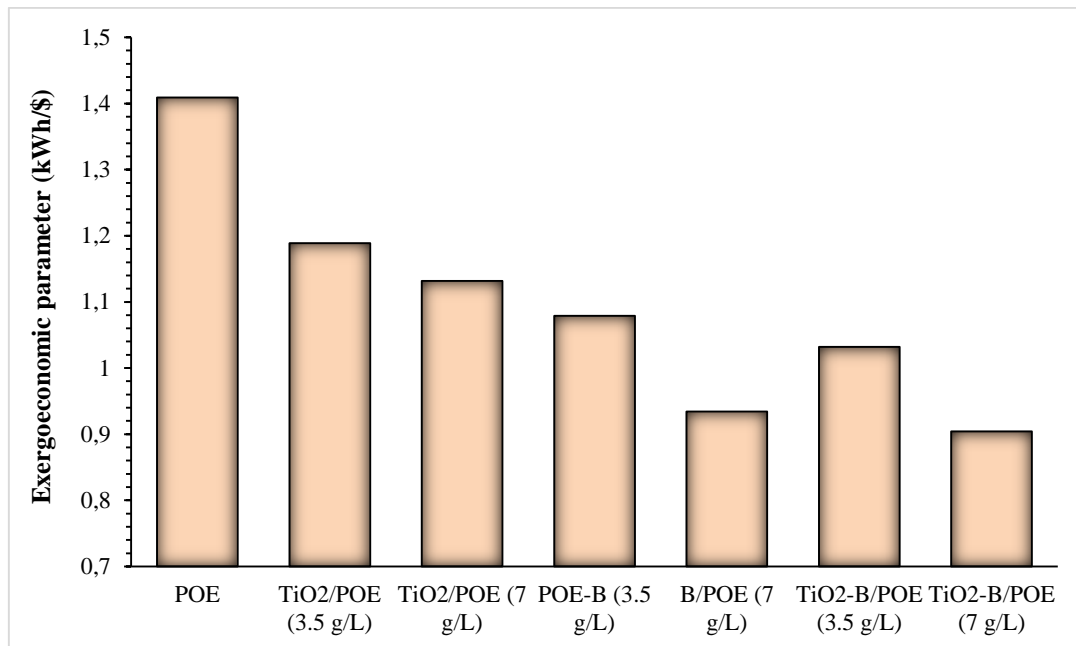
Figure 9. *Exergoeconomic values of mono and binary nanolubricants at different concentrations*

IV. CONCLUSION

In this study, different nanoparticles (TiO_2 and B) were added to the pure POE used in the VCRS at different concentrations (3.5 g/L and 7 g/L) to acquire mono and binary nanolubricants. The effects of the obtained mono and binary nanolubricants on the system performance were evaluated in terms of energy, exergy, environment and economy by comparing them with pure POE. Important details obtained as a result of the experiments are given below:

➢ Meaningful improvement was determined in mono and binary nanolubricants utilized in VCRS compared to POE. The highest COP increase was obtained as 16.47% in 7 g/L TiO_2-B nanolubricant compared to POE. It was determined that the COP value of the VCRS increased with the increase in the concentration of nanolubricants compared to POE.

➢ Mono and binary nanolubricants used in VCRSs have significantly reduced the energy consumption. Energy consumption increased by 13.06% in 7 g/L TiO_2-B binary nanolubricant compared to pure POE. This decreases the load on the compressor as nanolubricants decrease wear in the compressor and increase performance. Compressor efficiency is increased by using mono and binary nanolubricants.

➢ The total exergy destruction of the vapor-compression refrigeration system varies with the usage of mono and binary nanolubricants at different concentrations. As the concentration ratio enhances, the total exergy destruction of all mono and binary nanolubricants decreases while their exergy efficiency increases. Total exergy destruction decreased by 35.20% in 7 g/L TiO_2-B nanolubricant compared to POE.

➢ Exergy analysis in thermal energy systems is an important parameter to evaluate the usability of the system. In this way, improvements that can be made to the system can be seen. A meaningful increase in exergy efficiency was observed with the usage of mono and binary nanolubricants in the VCRS. Exergy efficiency was found to increase by 43.44% in 7 g/L TiO_2-B nanolubricant compared to pure POE.

> Exergoeconomic parameters of mono and binary nanolubricants utilized in VCRS were determined. Exergoeconomic parameter was improved by 35.84% in 7 g/L TiO$_2$-B binary nanolubricant compared to pure POE. Although B nanoparticle has a price 3-4 times more expensive than TiO$_2$ nanoparticle, it has lower economic performance because it increases system performance and causes a significant decrease in energy consumption.

> When mono and binary nanolubricants used in VCRSs were evaluated, they showed better performance than environmentally pure POE. This is because mono and binary nanolubricants reduce the energy consumption of the system, thus releasing less CO$_2$ into the environment. In environmental performance, 11.90% improvement was achieved in 7 g/L TiO$_2$-B binary nanolubricant compared to pure POE.

Nanofluids offer substantial advantages for enhancing VCRS performance. Nevertheless, there are benefits and drawbacks to nanofluids. One of the most significant drawbacks is that, after a while, nanofluids made using the one- or two-step approach sink to the bottom of the base fluid. As a result, the system cannot display the nanofluid's thermophysical characteristics. This is the main obstacle keeping the use of nanofluids in the refrigeration industry from becoming commercially viable. Furthermore, whereas binary and ternary nanofluids are used sparingly, mono nanofluids have been used extensively in previous research. Increasing the number of studies on this topic will improve the literature. Furthermore, there has been very few research on how the same sort of nanoparticles' size behave in systems. Increasing the number of these studies is critical for future research.

V. REFERENCES

[1]   D. C. Savitha, P. K. Ranjith, B. Talawar, and N. Rana Pratap Reddy, "Refrigerants for sustainable environment–a literature review," *International Journal of Sustainable Energy*, vol. 41, no. 3, pp. 235-256, 2022.

[2]   X. Cao, X. Dai, and J. Liu, "Building energy-consumption status worldwide and the state-of-the-art technologies for zero-energy buildings during the past decade," *Energy and Buildings*, vol. 128, pp. 198-213, 2016.

[3]   B. Citarella, L. Viscito, K. Mochizuki, and A. W. Mauro, "Multi-criteria (thermo-economic) optimization and environmental analysis of a food refrigeration system working with low environmental impact refrigerants," *Energy Conversion and Management*, vol. 253, pp. 115152, 2022.

[4]   A. Zendehboudi, A. Mota-Babiloni, P. Makhnatch, R. Saidur, and S. M. Sait, "Modeling and multi-objective optimization of an R450A vapor compression refrigeration system," *International Journal of Refrigeration*, vol. 100, ss. 141-155, 2019.

[5]   Á. R. Gardenghi, J. F. Lacerda, C. B. Tibiriçá, and L. Cabezas-Gomez, "Numerical and experimental study of the transient behavior of a domestic vapor compression refrigeration system–Influence of refrigerant charge and ambient temperature," *Applied Thermal Engineering*, vol. 190, pp. 116728, 2021.

[6]   M. W. Bhat, G. Vyas, A. J: Jaffri, and R. S. Dondapati, "Investigation on the thermophysical properties of Al$_2$O$_3$, Cu and SiC based Nano-refrigerants," *Materials Today: Proceedings*, vol. 5, no. 14, pp. 27820-27827, 2018.

[7]   M. Ghazvini, H. Maddah, R. Peymanfar, M. H. Ahmadi, and R. Kumar, "Experimental evaluation and artificial neural network modeling of thermal conductivity of water based nanofluid containing magnetic copper nanoparticles," *Physica A: Statistical Mechanics and its Applications*, vol. 551, pp. 124127, 2020.

[8]   A. Manoj Babu, S. Nallusamy, and K. Rajan, "Experimental analysis on vapour compression refrigeration system using nanolubricant with HFC-134a refrigerant," *Nano Hybrids*, vol. 9, pp. 33-43, 2016.

[9]   K. Martin, A. Sözen, E. Çiftçi, and H. M. Ali, "An experimental investigation on aqueous Fe–CuO hybrid nanofluid usage in a plain heat pipe," *International Journal of Thermophysics*, vol. 41, pp. 1-21, 2020.

[10]   M. N. M. Zawawi, W. H. Azmi, and M. F. Ghazali, "Performance of Al_2O_3-SiO_2/PAG composite nanolubricants in automotive air-conditioning system," *Applied Thermal Engineering*, vol. 204, pp. 117998, 2022.

[11]   S. S. Chauhan, "Performance evaluation of ice plant operating on R134a blended with varied concentration of Al_2O_3-SiO_2/PAG composite nanolubricant by experimental approach," *International Journal of Refrigeration*, vol. 113, pp. 196-205, 2020.

[12]   V. V. Wanatasanappan, M. Z. Abdullah, and P. Gunnasegaran, "Thermophysical properties of Al_2O_3-CuO hybrid nanofluid at different nanoparticle mixture ratio: An experimental approach," *Journal of Molecular Liquids*, vol. 313, pp. 113458, 2020.

[13]   N. N. M. Zawawi, W. H. Azmi, A. A. M. Redhwan, M. Z. Sharif, and K. V. Sharma, "Thermo-physical properties of Al_2O_3-SiO_2/PAG composite nanolubricant for refrigeration system," *International Journal of Refrigeration*, vol. 80, pp. 1-10, 2017.

[14]   N. Asokan, P. Gunnasegaran, and V. V. Wanatasanappan, "Experimental investigation on the thermal performance of compact heat exchanger and the rheological properties of low concentration mono and hybrid nanofluids containing Al_2O_3 and CuO nanoparticles," *Thermal Science and Engineering Progress*, vol. 20, pp. 100727, 2020.

[15]   A. Senthilkumar, E. P. Abhijith, and C. A. A. Jawhar, "Experimental investigation of Al_2O_3/SiO_2 hybrid nanolubriant in R600a vapour compression refrigeration system," *Materials Today: Proceedings*, vol. 45, pp. 5921-5924, 2021.

[16]   A. Senthilkumar, P. V. Abhishek, M. Adithyan, and A. Arjun, "Experimental investigation of CuO/SiO_2 hybrid nano-lubricant in R600a vapour compression refrigeration system," *Materials Today: Proceedings*, vol. 45, pp. 6083-6086, 2021.

[17]   A. Kumar and S. P. S. Rajput, "Energetic and exergetic analysis of a Vapour compression refrigeration test rig in varying concentrations of (TiO_2-SiO_2/MO) hybrid nano-lubricants and R600a refrigerant charges," *Energy Sources, Part A: Recovery, Utilization, and Environmental Effects*, vol. 45, no. 3, pp. 9118-9132, 2023.

[18]   M. J. Akhtar and S. P. S. Rajput, "Energy and exergy analysis of vapour compression test rig using R134a blended with GN-MWCNT/POE hybrid nano-lubricants," *Energy Sources, Part A: Recovery, Utilization, and Environmental Effects*, vol. 46, no. 1, pp. 188-208, 2024.

[19]   S. Govindasamy, M. Kaliyannan, S. Sadhasivam, and R. Kadasari, "Experimental analysis of domestic refrigeration system using nanorefrigerant [CeO_2+ ZnO+ R134a]," *Thermal Science*, vol. 26, no. (2 Part A), pp. 969-974, 2022.

[20]   R. Tripathi, G. N. Tiwari, and V. K. Dwivedi, "Overall energy, exergy and carbon credit analysis of N partially covered photovoltaic thermal (PVT) concentrating collector connected in series," *Solar Energy*, vol. 136, pp. 260-267, 2016.

[21]   Y. Su, Y. Zhang, and L. Shu, "Experimental study of using phase change material cooling in a solar tracking concentrated photovoltaic-thermal system," *Solar Energy*, vol. 159, pp. 777-785, 2018.

[22]   A. D. Tuncer, A. Khanlari, A. Sözen, E. Y. Gürbüz, C. Şirin, and A. Gungor, "Energy-exergy and enviro-economic survey of solar air heaters with various air channel modifications," *Renewable Energy*, vol. 160, pp. 67-85, 2020.

[23]   A. Kumar and A. Layek, "Energetic and exergetic performance evaluation of solar air heater with twisted rib roughness on absorber plate," *Journal of Cleaner Production*, vol. 232, pp. 617-628, 2019.

[24]   H. Hassan, M. S. Yousef, and S. Abo-Elfadl, "Energy, exergy, economic and environmental assessment of double pass V-corrugated-perforated finned solar air heater at different air mass ratios," *Sustainable Energy Technologies and Assessments*, vol. 43, pp. 100936, 2021.

[25]   A. R. Abd Elbar, M. S. Yousef, and H. Hassan, "Energy, exergy, exergoeconomic and enviroeconomic (4E) evaluation of a new integration of solar still with photovoltaic panel," *Journal of Cleaner Production*, vol. 233, pp. 665-680, 2019.

[26]   P. T. Saravanakumar, D. Somasundaram, and M. M. Matheswaran, "Exergetic investigation and optimization of arc shaped rib roughened solar air heater integrated with fins and baffles," *Applied Thermal Engineering*, vol. 175, pp. 115316, 2020.

[27]   S. S. Sanukrishna, M. Shafi, M. Murukan, and M. J. Prakash, "Effect of SiO_2 nanoparticles on the heat transfer characteristics of refrigerant and tribological behaviour of lubricant," *Powder Technology*, vol. 356, pp. 39-49, 2019.

[28]   S. S. Rawat, A. P. Harsha, and A. P. Deepak, "Tribological performance of paraffin grease with silica nanoparticles as an additive," *Applied Nanoscience*, vol. 9, pp. 305-315, 2019.

[29]   A. Singh, P. Chauhan, and T. G. Mamatha, "A review on tribological performance of lubricants with nanoparticles additives," *Materials Today: Proceedings*, vol. 25, pp. 586-591, 2020.